05,06,12

Microphase layering in PVDF composite–$CoFe_2O_4$ for printing with layering method

© P.A. Ershov[1], V.D. Salnikov[1], V.V. Savin[1], P.A. Vorontsov[1], L.V. Panina[1,2], V.V. Rodionova[1]

[1] Immanuel Kant Baltic Federal University,
Kaliningrad, Russia
[2] National University of Science and Technology „MISiS“,
Moscow, Russia

E-mail: pershov@kantiana.ru

Received November 30, 2024
Revised December 1, 2024
Accepted December 5, 2024

The microphase layering of the composite at the stage of filament yarn formation and its subsequent effect on FDM-printing (fusion deposition modelling) and properties of printed objects were studied. It was found that with the growth of the percentage content of nanoparticles in the filament, the dimensions of pores and ditches in the filament periphery increase. Appearance of defects in the polymer matrix with the increase of $CoFe_2O_4$ (CFO) concentration up to 15% is confirmed by differential-scanning calorimetry (DSC) — an additional peak is formed on the enthalpy variation curves. Despite the fact that the highest content of electroactive phase and the magnetization value were found in the film printed from filament thread with 15% content of CFO nanoparticles, the maximum magnetoelectric coefficient $\alpha_{33} = 3.2\,\text{mV}/(\text{cm} \cdot \text{Oe})$ was produced on the printed film with 10% content of CFO, which is due to microphase layering. The produced value of magnetoelectric coefficient is lower in the lamellar composites, however, it is sufficient for use of the composites in biomedicine, and use of the FDM-printing technology provides for the possibility of creating complex structures, such as cellular scaffolds.

Keywords: 3D-printing, multiferroics, functional composites, magnetic nanoparticles, fluoroplastic.

DOI: 10.61011/PSS.2024.12.60217.334

1. Introduction

This study is dedicated to the study of 3D-printing with functional polymer composites based on polyvinylidenfluoride (PVDF) with addition of $CoFe_2O_4$ (CFO) nanoparticles with concentrations 5, 10, 15 wt%. Additive technologies revolutionized in the methods of design and manufacturing, making it possible to develop unique properties based on complex geometry with high precision [1]. The most common 3D-printing technology was the technology of modeling with layering method (FDM, fused deposition modelling), making it possible to use thermoplastic polymers for design of objects with complex shape [2]. The key properties of the objects manufactured by 3D-printing methods, are the tensile strength, wear resistance and maximum operating temperatures.

Recently special attention has been paid to the development of 3D-printing technology using functional composites. Functional composites — are materials that combine the advantages of the traditional polymer materials with additional properties due to the filler additives, such as improved electroconductivity [3,4], magnetic properties [5,6], magnetoelectric properties [7,8]. Integrating functional materials in 3D-printing, you can create complex geometric shapes with individual properties, which may not be achieved by regular production methods [9].

One of the increasingly popular composite material, which is still poorly studied is PVDF with addition of magnetic nanoparticles. The interest is related to the synergy of piezoelectric and magnetostriction properties, which makes it possible to generate electric pulses by the external magnetic field [10]. The materials, where electric polarization is induced by magnetic field via mechanical connection of piezo- and magnetic components, are called magnetoelectric (ME) [11,12]. Efficiency of ME-bond in polymer composites with ferromagnetic nanoparticles as a filler initially depends on the piezoelectric and mechanical properties of the polymer matrix. ME-composites based on PVDF and CFO are the promising material for development of a new type of magnet-stimulating scaffolds for tissue engineering [8], ME-converters (to monitor human condition) [13] and flexible sensors [14,15].

However, when nanoparticles are added to the polymer matrix, often there is the effect of microphase layering with formation of heterogeneous structures at the microlevel between the nanoparticles and polymer [16,17]. This layering may arise as a result of differences in the chemical compatibility, thermal expandability and/or mechanical properties of the components. In case of PVDF, microphase layering may substantially impact electric and mechanical properties of the material [18,19]. At the same time, microphase layering may be used to achieve specific properties in the field of membrane technology or sensors [20,21], where PVDF is used thanks to its piezoelectric and dielectric properties [22].

This paper is dedicated to the study of 3D-printing with functional polymer composites based on polyvinylidenflu-

oride (PVDF) with addition of CFO nanoparticles with concentrations 5, 10, 15 wt%. The effect of microphase layering is studied, which is caused by segregation of CFO nanoparticles in the PVDF, to determine the optimal content of magnetic CFO nanoparticles with the purpose to maximize the magnetoelectric response of the printed object.

2. Test specimens and experimental procedure

The following reagents were used in the paper: $Co(NO_3)_2 \cdot 6H_2O$ ($\geq 98\%$; LenReaktiv, St. Petersburg, Russia), $Fe(NO_3)_3 \cdot 9H_2O$ ($\geq 98\%$; LenReaktiv, St. Petersburg, Russia), citric acid ($\geq 98\%$; LenReaktiv, St. Petersburg, Russia), ammonia solution 30% ($\geq 98\%$; SigmaTek, Khimki, Russia), N,N-dimethyl formamide ($\geq 98\%$; Ekos-1, Moscow, Russia) PVDF, 80000 mol (GaloPolimer, Moscow, Russia).

Magnetic CFO nanoparticles were produced using the method of sol-gel-self-combustion [23]. To produce CFO, metal salts were taken at molar ratio of $Co_2^+ : Fe_3^+ = 1 : 2$. M-solution of citric acid was added to M-aqueous solution of salts with the same volume. pH level was made up to ~ 7 by addition of ammonia liquor. The produced solutions were heated at 150°C at intense mixing to achieve gel-like state. The self-combustion reaction was initiated by temperature increase to 300°C. The reaction product was ground in agate mortar and washed several times by distilled water and acetone. The average time of the produced crystallites does not exceed 20 nm [24].

PVDF granules are dissolved in dimethylformamide (DMF) at 40°C with continuous mixing until complete dissolution of the polymer initial mixture with the mass ratio of 1:6. The total concentration of PVDF to DMF was corrected to 1:8 by introduction of particle suspension. The end mass concentration of particles in the composite is equal to 5, 10, 15%.

The thin composite film of PVDF-CFO was formed using doctor blade technique [25]. The polymer solution was placed on the substrate in front of the moving blade, which distributed the solution on the substrate surface. The layer thickness was specified at level 100 μm by adjustment of a clearance between the knife and the substrate.

A composite PVDF-CFO thread was created by extrusion of a ground film produced at the previous stage. Extrusion was performed using microextruder Twin Tech Screw (Rondol). Extrusion temperature was 220°C. Extruder rotation speed was 12 rpm. The extruded thread was cooled down at room temperature. The thread produced at the initial and final stages of extrusion was rejected. A round die was used for the extrusion process with diameter of 1.75 mm, suitable for FDM-printing.

For 3D-printing with extruded composite threads, FDM-printer Creality Ender 3 Pro with a nozzle of 0.4 mm diameter was used. 3D-printing was performed at extruder temperature 290°C and table temperature 100°C. Printing speed was 20 mm/s. For the study, the square films were printed with thickness of 0.12 mm and dimensions of 10×10 mm with concentric filling.

To study the nanocomposite surface, a scanning electron microscope (SEM, Hitachi TM4000 Plus) was used in the electron backscattering mode.

Differential scanning calorimetry (DSC, NETZSCH 204 F1 Phoenix) was used to assess the degree of specimen crystallinity, by comparing the melting heat of the specimen and the fully crystallized PVDF (104.6 J/g) [26]. The specimens were analyzed in the interval from the room temperature to 200°C at heating speed 5°C/min in the argon atmosphere. The degree of crystallinity χ was calculated from equation

$$\chi = \frac{\Delta H}{H_{100}\varphi_{\text{PVDF}}} \times 100\%,$$

where ΔH — melting heat, H_{100} — enthalpy for 100% crystalline phase of PVDF, φ_{PVDF} — mass concentration of PVDF.

IR spectra were obtained using IR-Fourier-spectrometer (Simex FT-801 IR). The produced filaments and printed composite PVDF-CFO films were studied using the method of the attenuated total reflection (ATR) in the range of wave numbers from 4000 to 600 cm^{-1}. The specimens were placed on a diamond prism and pressed to ensure the maximum contact between the surfaces. IR spectra were read from 3 areas on the sample, and then averaged. The number of electroactive FEA phase was assessed using equation [27]

$$F_{\text{EA}} = \frac{I_{\text{EA}}}{(K_{840}/K_{763})I_{763} + I_{\text{EA}}} \times 100\%,$$

where I_{763} and I_{EA} — absorption intensities at characteristic wave numbers 763 and 840 cm^{-1}; K_{840} and K_{763} — corresponding absorption coefficients.

Field dependences of magnetization for all specimens are measured on vibration magnetometer (Lakeshore 7400 System) in fields up to 12 kOe at room temperature. Specimens of threads and films (5×5 mm) were fixed in the orientation, when the magnetic field is perpendicular to the plane of the films. The CFO nanoparticle hysteresis loop measurement results are presented in paper [28].

Measurement of the magnetoelectric coefficient α_{33} in the orientation of the composite, when the direction of the external magnetic field (both permanent and alternating) matches the direction of polarization inside the specimen, was carried out by dynamic method [29,30]. Permanent magnetic field, where the specimen was placed, was created using electromagnets of vibration magnetometer (7400 System VSM; Lake Shore Cryotronics Inc). Weak alternating magnetic field H_{AC} with the value of up to 1.5 Oe and frequency of 770 Hz was developed using Helmholtz coils. The difference of potentials V_{out}, created between the surfaces of the specimen, was detected with the help

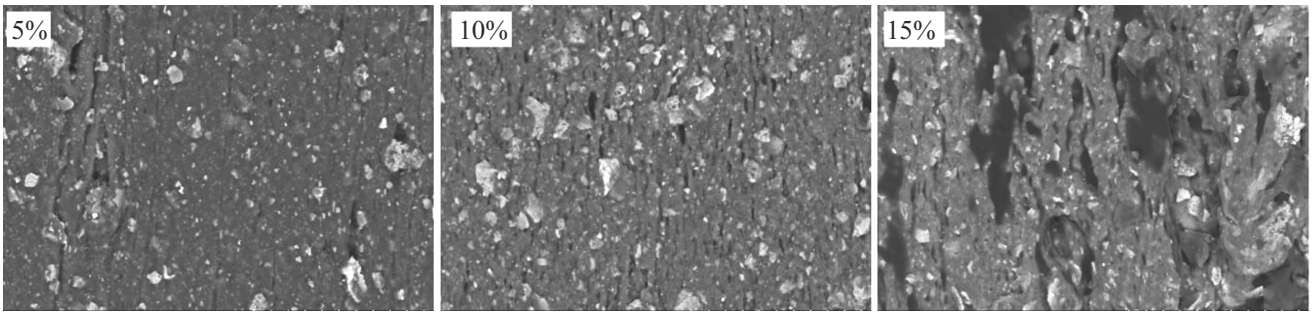

Figure 1. SEM-images of PVDF/CFO filaments with different content of nanoparticles: 5, 10 and 15 wt%.

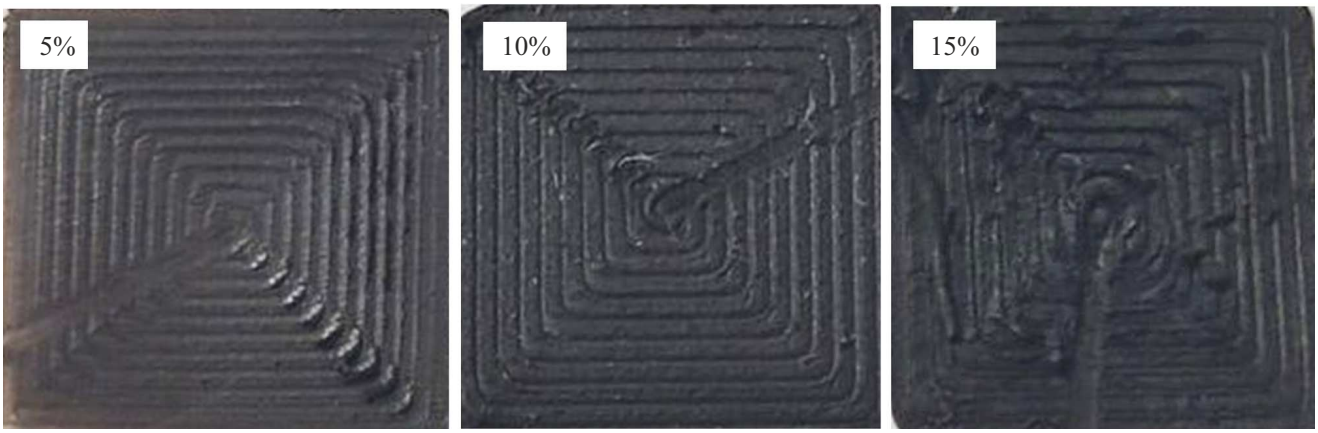

Figure 2. Photo of printed films, with dimensions of 10×10 mm, filled concentrically.

of lock-in amplifier SR 830 (Stanford Research Systems). The value of the magnetoelectric coefficient was calculated using formula

$$\alpha_{33} = \frac{V_{\text{out}}}{tH_{\text{AC}}},$$

where t — specimen thickness. Specimen thicknesses were measured using a micrometer.

3. Experimental results and discussion thereof

As one can see on SEM-images of the filaments (Figure 1), microphase layering results in deterioration of the composite integrity. Ditches and pores are extended and directed towards the filament extension sides. Layering appears at CFO particle concentration of 10%. Their size changes from $\sim 3\,\mu$m for 10% particle content to a dozen of microns at 15% CFO content. Besides, the images also contain agglomerates of nanoparticles (NPs) with dimensions from 3 to $20\,\mu$m, which also influence the processes of microphase layering and are caused by segregation of the particles and their accumulation at the stages of filament production.

As a result, during FDM-printing with PVDF-CFO composite the microphase layering on the filament causes defects—beads, as one can see on the photos of printed films (Figure 2).

SEM-images of the smooth side of printed films (Figure 3) contain a microtexture only on the film printed with 15% content of CFO nanoparticles, which means that the microphase layering of the polymer is transferred from the filament to the printed film.

The analysis of the curves of differential scanning calorimetry (DSC) (Figure 4) found that in the films with nanoparticle content of 10 and 15% the degree of crystallinity decreased compared to the specimen, where the NP content was 5%, at the same time the melting temperature would not change (see Table 1).

Decrease in the degree of crystallinity is explained by the larger agglomeration of NPs at concentrations of 10 and 15 wt%. NP agglomerates disturb the process of crystallization, which in its turn prevents leveling and ordered position of polymer chains [31]. Besides, the DSC curve for the printed specimen with 15% NP content demonstrates peak splitting. As the NP concentration increases, dimensions of agglomerates increases in the polymer matrix, which is a defect for the polymer matrix, which may cause various phase transitions during heating.

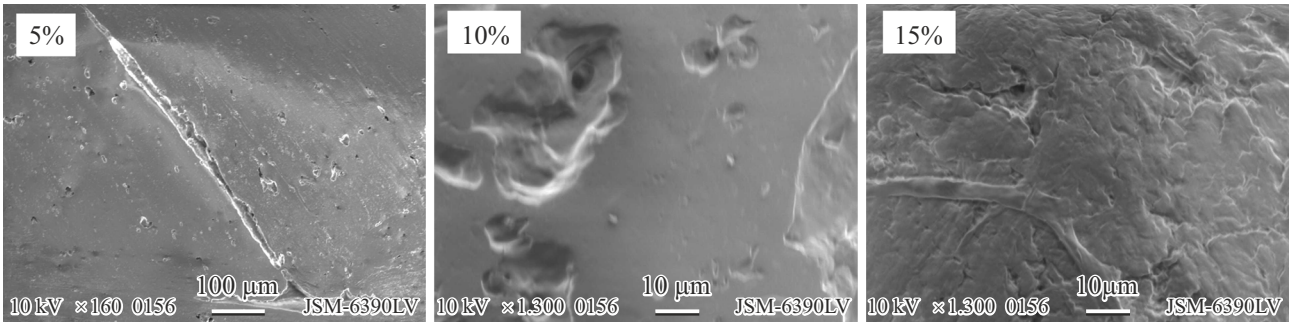

Figure 3. SEM-image of smooth side of printed film adjacent to glass during 3D-printing with PVDF-CFO composite.

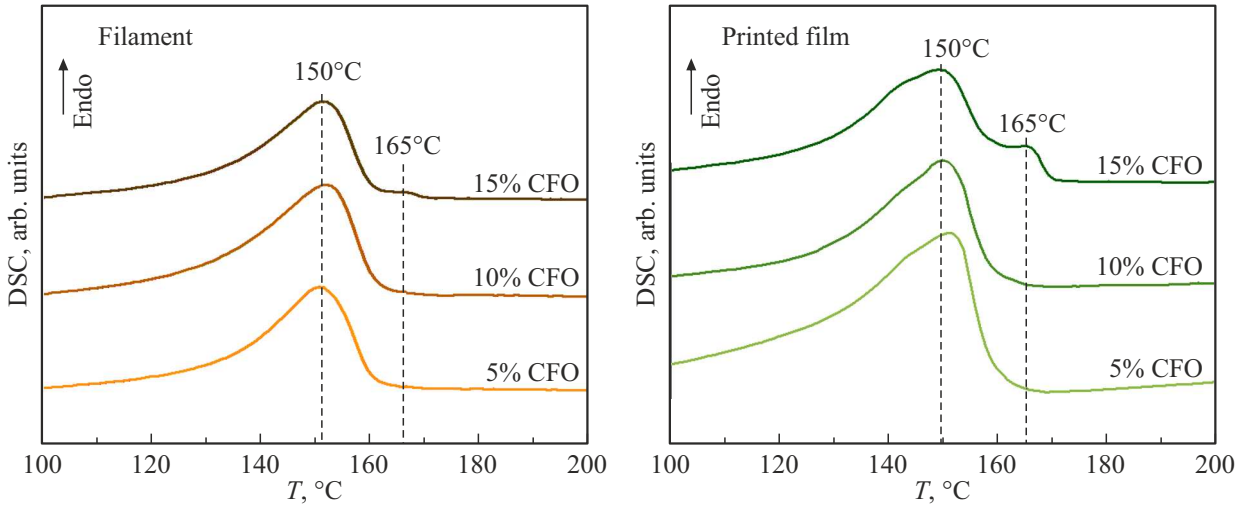

Figure 4. DSC-curves for PVDF-CFO composite films with different content of CFO particles: 5–15%.

Table 1. Calculated values of crystallinity χ for filaments and printed films

Specimen	χ, % for filament	χ, % for printed films
PVDF-5% CFO	31	63
PVDF-10% CFO	39	40
PVDF-15% CFO	35	46

Therefore, the interaction between the NP agglomerates and PVDF matrix may change the crystallization process, therefore, various crystalline forms may be created, which are observed as melting peak splitting, which may also mean formation of electroactive phase $(\beta + \gamma)$ [32].

To study the effect of layering at phase composition of the composite, IR spectrometry was performed of both the obtained filaments and the printed composite films (Figure 5). The share of electroactive phase in the extruded composite filaments remains invariable within the statistic spread of this value — $87 \pm 2\%$.

After 3D-printing the quantity of electroactive phase decreases (which was determined using the specific peak on wave number $840\,cm^{-1}$), however, the least variation of the electroactive phase quantity after printing is observed on a specimen with 15% CFO nanoparticle content. One may conclude that the presence of layering positively influences the formation of electroactive phase during FDM-printing.

The drop of the share of electroactive phase after FDM-printing may be explained by the process of polymer melting without subsequent extrusion of the melt, which results in a more stable alpha phase of PVDF.

The measured magnetic characteristics of the composites and the main magnetic parameters are provided in Table 2.

The values of saturation magnetization M_s of composite films agree with the specified nanoparticle content, except for PVDF-15% CFO specimen. The relative residual magnetization (M_r/M_s) for all specimens was around 30%, which is below the expected value for the non-interacting single-domain particles according to Stoner–Wohlfarth model [33].

The observed value of coercive force H_c for the composites is higher than for the particles. Such nature of change H_c may indicate the effect of interparticle interaction

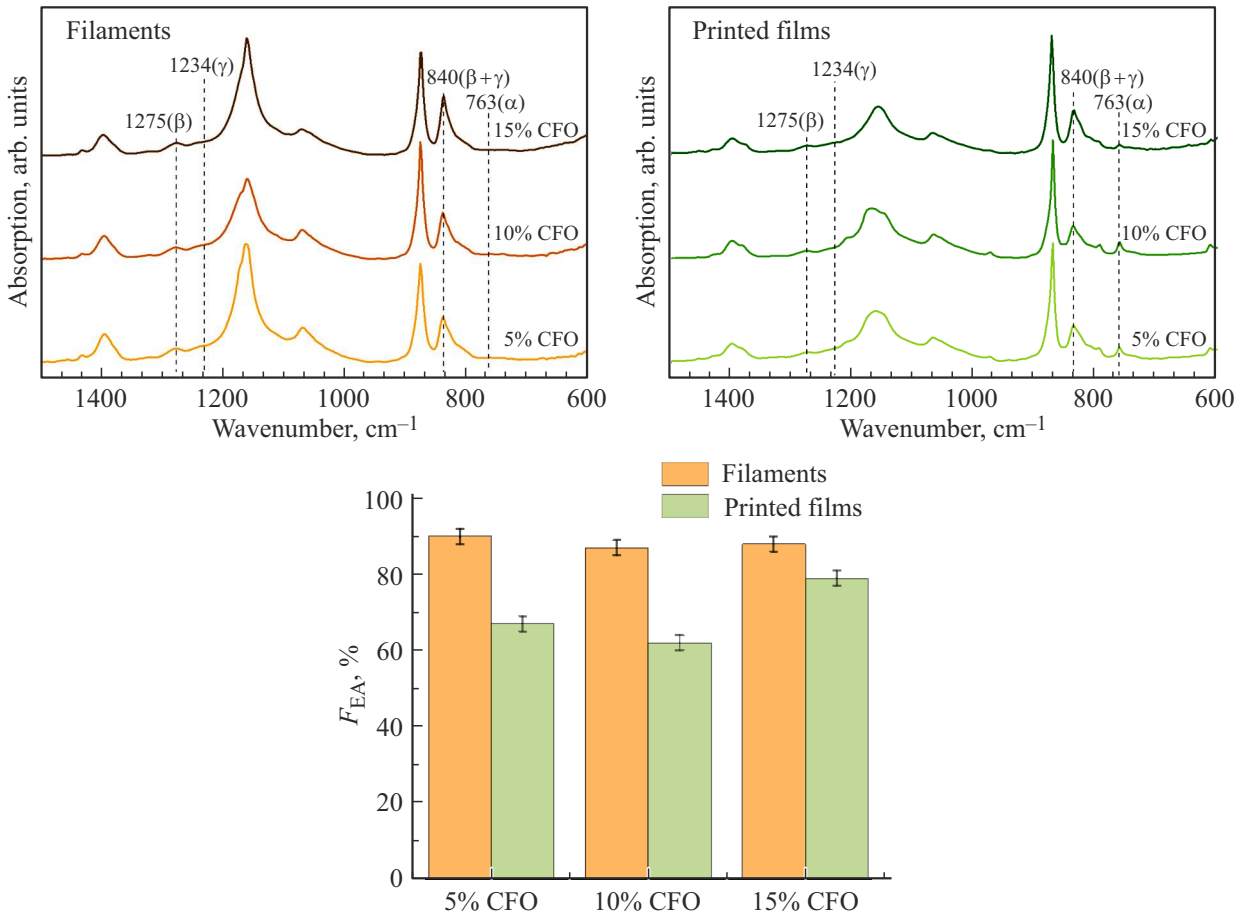

Figure 5. IR-spectra of filaments (left) and printed films (right). See below the calculated quantity of electroactive phase using the obtained spectra.

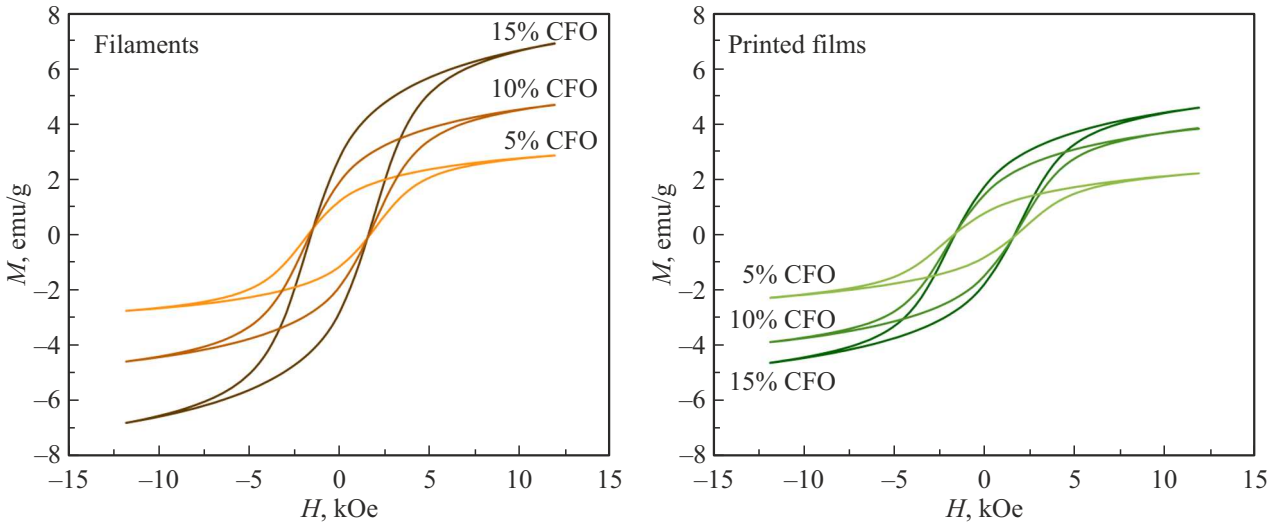

Figure 6. Field dependence of magnetization M for filament thread (left) and films printed with composite (right).

Table 2. Measured magnetic characteristics of composites

		H_c, kOe	M_s, emu/g	M_r/M_s	%
CFO		1.46	47	0.29	100
PVDF-15% CFO	filament	1.59	8.4	0.32	17
	film	1.63	5.7	0.30	12
PVDF-10% CFO	filament	1.64	5.6	0.33	11
	film	1.66	4.7	0.30	10
PVDF-5% CFO	filament	1.72	3.4	0.34	7
	film	1.72	2.9	0.27	6

Table 3. Measured magnetoelectric parameters of printed films

Concentration of CFO particles in composite film, %	α_{33}, mV/(cm · Oe)
5	2.0 ± 0.1
10	3.2 ± 0.2
15	1.8 ± 0.1

due to the change in the interparticle distance in the matrix, i.e. on agglomeration reduction [34]. Besides, increased concentration of particles causes formation of larger agglomerates, which causes reduction of H_c. It is interesting that in the composite after printing the particles are less aggregated than in the filament thread, i.e. the particles are redistributed as a result of thread extrusion in process of printing.

Magnetoelectric coefficient α_{33} was measured on composite films with size of 10×10 mm, thickness of 200 μm. The maximum values of magnetoelectric coefficient for the studied composites were presented in Table 3.

It was found that the film with 10% CFO has the highest magnetoelectric coefficient. Reduction of the magnetoelectric coefficient in the film with 15% CFO may be due to the microphase layering, which prevents homogeneous transfer of mechanical stresses. Besides, agglomeration of CFO particles with their concentration increase reduces the cohesion of the composite components.

4. Conclusion

The technology of 3D-printing with functional polymer composites, including with magnetic nanoparticles, opens new opportunities for management of both the shape of the objects and their properties. However, addition of nanoparticles into the polymer matrix may cause unwanted processes of polymer destruction.

The effect of microphase layering of PVDF-CFO composite was studied, which was observed at the stage of filament thread production for FDM-printing, as well as its effect on the properties of the printed object. Analysis of composites with 5, 10, 15 wt% content of cobalt ferrite (CFO) nanoparticles found that ditches and pores were present in the filament periphery, dimensions of which increase with NP content. Analysis of DSC curves showed that filaments and printed films with 15% content of nanoparticles demonstrate an additional peak, which may be referred to appearance of defects in the polymer matrix. Analyzing the quality of PVDF-CFO films produced by FDM-printing method, one may conclude that the microphase layering causes appearance of printing defects — beads. According to the data of IR-spectrometry, the quantity of electroactive phase, despite the layering, did not change for the filaments and is $87 \pm 2\%$ with account of statistical dispersion. Transformation of the phase composition upon transfer to the printed object for the specimens with different share of CFO particles happens differently. The largest share of electroactive phase was found in the printed film with 15% nanoparticle content, therefore, one may conclude on the favorable effect of the polymer layering on the electroactive phase development. Nevertheless , measurements of magnetoelectric properties demonstrated that the highest values of the magnetoelectric coefficient 3.2 mV/(cm · Oe) are achieved at 10% content of CFO nanoparticles. This is due to the fact that the process of phase layering that increases with the increase of CFO concentration disturbs the mechanical cohesion of components. Therefore, one may conclude that the optimal quantity of CFO NPs for provision of magnetoelectric properties of composite films printed with FDM method is 10%, and FDM-printing as such does not make it possible to prevent microphase layering, observed at the stage of the filament thread. The produced values of magnetoelectric coefficient are sufficient for using the printed composites for magnetoelectric stimulation in biomedical applications, for example, in regenerative medicine, and 3D-printing capabilities make it possible to recreate the necessary complex forms for the cellular scaffolds.

Acknowledgments

The authors would like to thank A.A. Amirova for making filaments, A.S. Omelianchik for making nanoparticles, G.V. Kirichuk for his valuable contribution to measurements with the help of SEM.

Funding

The studies were performed with the financial support from the Russian Science Foundation under project No. 21-72-30032.

Conflict of interest

The authors declare that they have no conflict of interest.

References

[1] L. Zhou, J. Miller, J. Vezza, M. Mayster, M. Raffay, Q. Justice, Z. Al Tamimi, G. Hansotte, L.D. Sunkara, J. Bernat. Sensors **24**, *9*, 2668 (2024).

[2] R. Kristiawan, F. Imaduddin, D. Ariawan, U. Sabino, Z. Arifin. Open Engineering **11**, *1*, 639 (2021).

[3] J. Yang, N. Li, J. Shi, W. Tang, G. Zhang, F. Zhang. Multimaterial 3D Printing Techology. Elsevier (2021). P. 113−152.

[4] G. Cao, S. Cai, H. Zhang, Y. Chen, Y. Tian. ACS Appl. Polym. Mater. **4**, *5*, 3352 (2022).

[5] Q. Lu, K. Choi, J.-D. Nam, H.J. Choi. Polymers (Basel) **13**, *4*, 512 (2021).

[6] S. Salem, E. Yilmaz. In: Magnetic Nanoparticle-Based Hybrid Materials: Fundamentals and Applications / Eds A. Ehrmann, M. Ahmadi, A. Farmani, P. Nguyen-Tri, T.A. Nguyen. Elsevier (2021). P. 139−182.

[7] A. Sasmal, A. Arockiarajan. Nano Energy **115**, 108733 (2023).

[8] A. Omelyanchik, V. Antipova, C. Gritsenko, V. Kolesnikova, D. Murzin, Y. Han, A.V. Turutin, I.V. Kubasov, A.M. Kislyuk, T.S. Ilina, D.A. Kiselev, M.I. Voronova, M.D. Malinkovich, Y.N. Parkhomenko, M. Silibin, E.N. Kozlova, D. Peddis, K. Levada, L. Makarova, A. Amirov, V. Rodionova. Nanomater. **11**, *5*, 1154 (2021).

[9] Y. Wang, B. Jia, S. Liu, X. Yao, C. Sun. In: Advances in Transdisciplinary Engineering **22**. IOS Press (2022). P. 128−138. https://doi.org/10.3233/ATDE220220

[10] J.-W. Zhang, H.-Y. Guo, X. Chen, R.-T. Liu. In: Magnetoelectric Polymer−Based Composites. Wiley (2017). P. 1−12.

[11] L.A. Makarova, D.A. Isaev, A.S. Omelyanchik, I.A. Alekhina, M.B. Isaenko, V.V. Rodionova, Y.L. Raikher, N.S. Perov. Polymers (Basel) **14**, *1*, 153 (2022).

[12] P. Martins, S. Lanceros-Méndez. Adv. Funct. Mater. **23**, *27*, 3371 (2013).

[13] K. Maity, D. Mandal. In: Woodhead Publishing in Materials, Advanced Lightweight Multifunctional Materials. Woodhead Publishing (2021). P. 239−282.

[14] T. Li, Z. Xu, B.B. Xu, Z. Guo, Y. Jiang, X. Zhang, M. Bayati, T.X. Liu, Y.-H. Liu. Nano Res. **16**, *7*, 10493 (2023).

[15] L. Zhang, S. Li, Z. Zhu, G. Rui, B. Du, D. Chen, Y.-F. Huang, L. Zhu. Adv. Funct. Mater. **33**, *38*, 2301302 (2023).

[16] E. Koumoulos, E. Gkartzou, C.A. Charitidis. Manufact. Rev. **4**, 12 (2017). https://doi.org/10.1051/mfreview/2017012

[17] C. Liu, Q. Li, W. Kang, W. Lei, X. Wang, C. Lu, M. Naebe. J. Mater. Chem. A **10**, *1*, 10 (2022).

[18] U.O. Uyor, A.P. Popoola, O. Popoola, V.S. Aigbodion. Adv. Polymer Technol. **37**, *8*, 2838 (2018).

[19] F. Liu, N.A. Hashim, Y. Liu, M.R.M. Abed, K. Li. J. Membrane Sci. **375**, 1 (2011).

[20] N. Zhu, J. Zhou, L. Zhang, N. Yao, D. Dastan, J. Zhang, Y. Chen, X. Zhang. Soft Matter **19**, *24*, 4401 (2023).

[21] C. Li, S.M. Meckler, Z.P. Smith, J.E. Bachman, L. Maserati, J.R. Long, B.A. Helms. Adv. Mater. **30**, *8*, 1704953 (2018).

[22] S. Yempally, E. Kacem, D. Ponnamma. Discover Nano **18**, *1*, 93 (2023).

[23] C. Cannas, A. Falqui, A. Musinu, D. Peddis, G. Piccaluga. J. Nanoparticle Res. **8**, *2*, 255 (2006).

[24] A. Amirov, A. Omelyanchik, D. Murzin, V. Kolesnikova, S. Vorontsov, I. Musov, K. Musov, S. Khashirova, V. Rodionova. Processes **10**, *11*, 2412 (2022).

[25] C. Ribeiro, C.M. Costa, D.M. Correia, J. Nunes-Pereira, J. Oliveira, P. Martins, R. Gonçalves, V.F. Cardoso, S. Lanceros-Méndez. Nature Protoc. **13**, *4*, 681 (2018).

[26] F. Orudzhev, S. Ramazanov, D. Sobola, P. Kaspar, T. Trčka, K. Částková, J. Kastyl, I. Zvereva, C. Wang, D. Selimov, R. Gulakhmedov, M. Abdurakhmanov, A. Shuaibov, M. Kadiev. Nano Energy **90**, *Part B*, 106586 (2021).

[27] X. Cai, T. Lei, D. Sun, L. Lin. RSC Adv. **7**, *25*, 15382 (2017).

[28] V. Antipova, A. Omelyanchik, K. Sobolev, S. Pshenichnikov, S. Vorontsov, E. Korepanova, D. Schitz, D. Peddis, L. Panina, K. Levada, V. Rodionova. Polymer (Guildf) **290**, 126567 (2024).

[29] M. Mahesh Kumar, A. Srinivas, S.V. Suryanarayana, G.S. Kumar, T. Bhimasankaram. Bull. Mater. Sci. **21**, *3*, 251 (1998).

[30] M.H. Amiri, H. Sharifi Dehsari, K. Asadi. J. Appl. Phys. **132**, *16*, 164102 (2022).

[31] D. Petrukhin, V. Salnikov, A. Nikitin, I. Sidane, S. Slimani, S. Alberti, D. Peddis, A. Omelyanchik, V. Rodionova. J. Composites Sci. **8**, *8*, 329 (2024).

[32] N. María, Y. Patil, G. Polymeropoulos, A. Peshkov, V. Rodionov, J. Maiz, N. Hadjichristidis, A.J. Müller. Eur. Polym. J. **179**, 111506 (2022).

[33] E.C. Stoner, E.P. Wohlfarth. Philosophical Trans. Royal Soc. London. Series A, Mathematical and Physical Sciences **240**, *826*, 599 (1948).

[34] S. Slimani, A. Talone, M. Abdolrahimi, P. Imperatori, G. Barucca, D. Fiorani, D. Peddis. J. Phys. Chem. C **127**, *18*, 8840 (2023).

Translated by M.Verenikina